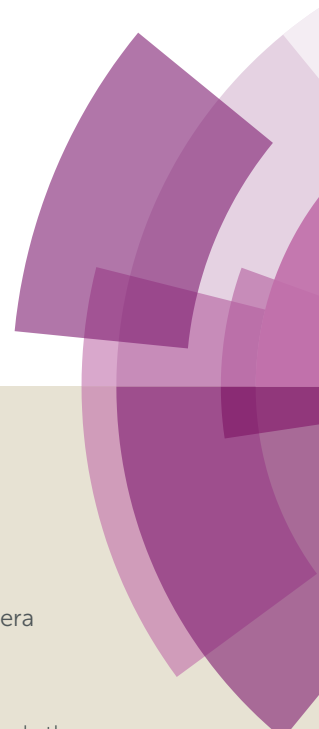


Dalton Transactions

Accepted Manuscript



This article can be cited before page numbers have been issued, to do this please use: P. Arce, C. M. Vera, D. L. Escudero, J. Guerrero, A. G. Lappin, A. G. Oliver, D. H. Jara, G. Ferraudi and L. A. Lemus, *Dalton Trans.*, 2017, DOI: 10.1039/C7DT02244A.



This is an Accepted Manuscript, which has been through the Royal Society of Chemistry peer review process and has been accepted for publication.

Accepted Manuscripts are published online shortly after acceptance, before technical editing, formatting and proof reading. Using this free service, authors can make their results available to the community, in citable form, before we publish the edited article. We will replace this Accepted Manuscript with the edited and formatted Advance Article as soon as it is available.

You can find more information about Accepted Manuscripts in the [author guidelines](#).

Please note that technical editing may introduce minor changes to the text and/or graphics, which may alter content. The journal's standard [Terms & Conditions](#) and the ethical guidelines, outlined in our [author and reviewer resource centre](#), still apply. In no event shall the Royal Society of Chemistry be held responsible for any errors or omissions in this Accepted Manuscript or any consequences arising from the use of any information it contains.

Structural diversity in Cu(I) complexes of the PNP ligand: from pincer to binuclear coordination modes and their effects upon the electrochemical and photophysical properties.

Pablo Arce,[†] Cristian Vera,[†] Dayra Escudero,[†] Juan Guerrero,[†] Alexander Lappin,[§] Allen Oliver,[§] Danilo H. Jara,^{≠,§} Guillermo Ferraudi,^{≠,§} Luis Lemus.^{†*}*

[†]Facultad de Química y Biología, Universidad de Santiago de Chile, Av. Libertador Bernardo O'Higgins 3363, Estación Central, Santiago, Chile.

[§]Department of Chemistry and Biochemistry, University of Notre Dame, Notre Dame, IN 46556-5670, USA.

[≠]Radiation Research Building, University of Notre Dame, Notre Dame, Indiana 46556, USA.

ABSTRACT

A set of new copper (I) complexes is synthesized and characterized using a labile PNP pincer ligand (PNP=N,N'-bis(diphenylphosphine)-2,6-diaminopyridine). A homoleptic Cu(I) complex $[\text{Cu}(\text{PNP}-\kappa\text{P}^I:\kappa\text{N}^I)_2]^+$, (**1**), was prepared, and taking advantage of the uncoordinated phosphorus atoms in (**1**), reaction with a second Cu(I) atom bearing secondary ligands (PPh₃, phen or dmp) allows the formation of new complexes: A bimetallic helicate $[\text{Cu}_2^I(\text{PNP})_2(\text{phen})]^{2+}$, (**2**), a mononuclear pincer complex $[\text{Cu}^I(\text{PNP})(\text{PPh}_3)]^+$, (**3**), and a heteroleptic complex $[\text{Cu}^I(\text{PNP})(\text{dmp})]^+$, (**4**). All complexes were characterized by X-ray crystallography, NMR (VT-NMR for (**1**) and (**4**)), cyclic-voltammetry, and steady-state and time-resolved luminescence spectroscopy. The fluxional behavior in (**1**) was studied by ³¹P VT-NMR, where an E_a value of 47.42 kJ/mol was calculated for the intramolecular alternating coordination of -PPh₂ moieties in PNP to the metal atom. This set of compounds reveals the versatility of the PNP ligand when added to the coordinating properties of Cu(I). The four complexes exhibit emission in solution and complexes (**2**)-(4) display intense luminescence in the solid state. The oscillographic traces showing the decay of the luminescence were fitted to biexponential functions with time constants: $8.0 \mu\text{s} > \tau_{\text{em},1} > 0.37 \mu\text{s}$ and $50 \mu\text{s} > \tau_{\text{em},2} > 2.2 \mu\text{s}$ for complexes (**2**), (**3**) and (**4**), respectively. Radiative relaxation is associated with electronic transitions in both the ligand PNP and metal-to-ligand charge transfer (MLCT).

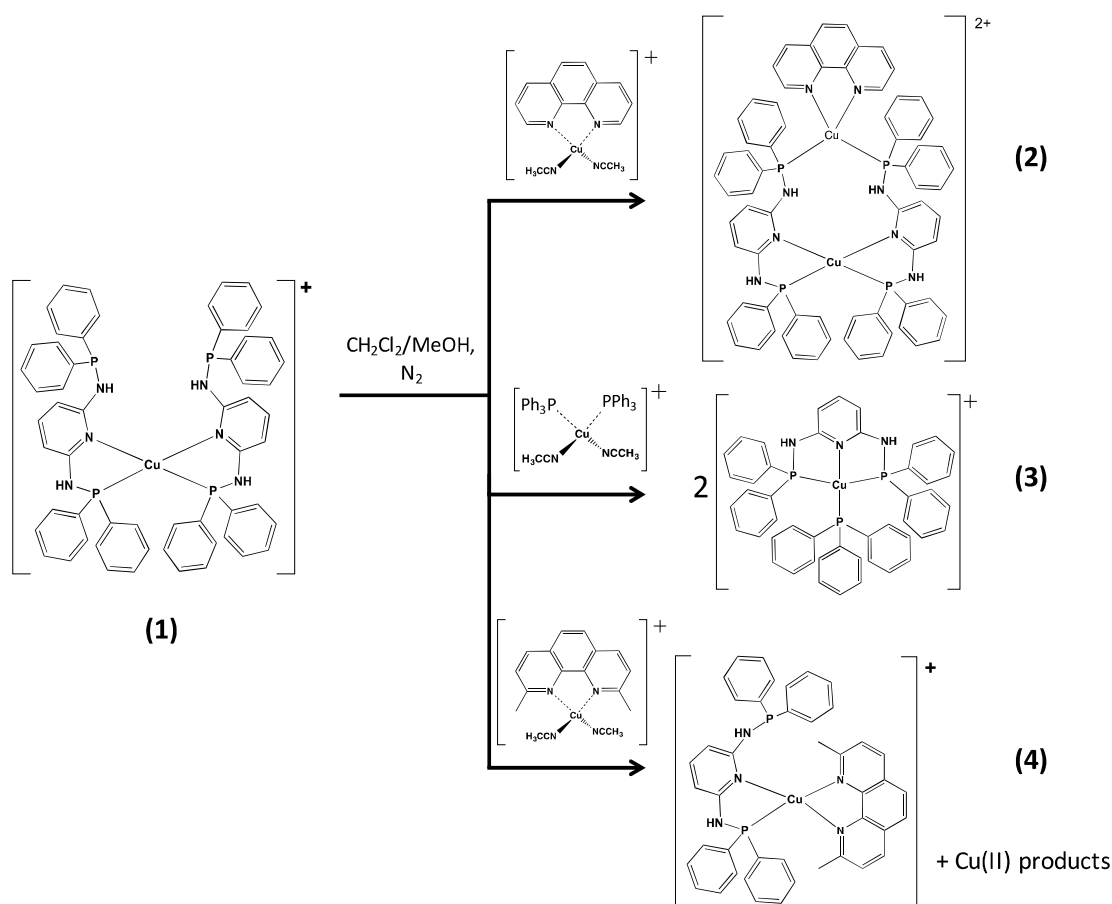
INTRODUCTION

New PNP complexes of Cu(I) have been investigated in this work to establish their solid and solution phase structures including the energetic parameters associated with the fluxional behavior and photophysical properties. PNP is regarded as one of various tridentate pincer ligands, namely ligands whose name is associated with the coordination mode to transition metal ions. Their general structural features are a central pyridine or phenyl ring *ortho*-disubstituted by two coordinating moieties, usually having N or P donor atoms. Since the synthesis of the first pincer complexes in the early 1970s,¹⁻³ they have found several applications in chemistry, including catalysis,⁴ sensors and the building of supramolecular architectures.⁵

By far, the chemistry of pincer complexes has been related to the platinum group and metals such as Ni, Fe and Mo due to their catalytic properties. Complexes of coinage metals have been received lesser attention. In particular, there is a limited amount of work based on Cu(I)-pincer complexes.⁶⁻¹¹ In the preparation of the Cu(I) complexes a main difficulty is that the ideal tetrahedral geometry of the copper(I) ion works against the coplanarity of the donor atoms in PNP. Therefore, the pincer coordination of PNP or NNN ligands to Cu(I) (P and N are nitrogen and phosphorus atoms coordinating to copper cation) results in the formation of mononuclear complexes with the geometry of a highly distorted tetrahedron. In solution phase, the lability of the d^{10} copper(I) atom when combined with the structural rigidity imposed by a tridentate pincer ligand leads to fluxional behavior where the ligand is bidentate with a rapid intramolecular rearrangement.^{11, 12} The versatility of pincer ligands with multiple binding sites and PNP, PNN or NNN as donor atoms, combined with the geometrical preferences of d^{10} metals¹⁰ is a useful tool in the preparation of new bimetallic complexes with the ligands bridging to both metal

centers.¹³ Although the designation of “pincer” ligand is the result of the mode of coordination to the metal center, this family of tridentate ligands offers more possibilities of coordination number, nuclearity and geometries around the metal center.¹⁴

With the focus on the preparation of new bimetallic complexes, we have taken advantage of the uncoordinated phosphorus atoms in $[\text{Cu}(\text{PNP}-\kappa P^I:\kappa N^I)_2]^+$ (**1**), Scheme I, to add a second copper atom that is also coordinated to a secondary ligand; PPh_3 , phenanthroline or neocuproine. Using this approach, three new different compounds were obtained under similar synthetic methods (**2**) – (**4**), Scheme I, where the PNP ligand is coordinating in different modes depending on the other ligand to produce either a bimetallic helicate (**2**), a mononuclear pincer complex (**3**) or a heteroleptic complex (**4**). The complexes (**2**), (**3**) and (**4**) present an intense luminescence in the solid phase which make them attractive materials for light-emitting devices. The structures of this set of complexes are fully characterized by X-ray crystallography and in solution by NMR (VT-NMR). The electrochemical behavior is studied by cyclic-voltammetry. In addition, photophysical properties of the complexes were evaluated both in solution and solid phase, and are discussed as a function of their structures, opening potential applications in areas such as luminescent devices, sensors and bio-applications.^{15,16}



Scheme I. Representation of products obtained (2-4) by direct reaction of the precursor (1) with heteroleptic Cu(I) complexes of phen, PPh_3 and dmp. For complex (4), a second procedure described in the methodology section can be followed with improved yielding.

EXPERIMENTAL SECTION

Materials

Chlorodiphenylphosphine (PPh_2Cl), 1,10-phenanthroline (phen), 2,9-dimethyl-1,10-phenanthroline (dmp) and triphenylphosphine (PPh_3) were from Sigma-Aldrich or Merck and used as received. Triethylamine (Et_3N) was dried by distillation over KOH pellets and other solvents were dried by their respective procedures. Commercial 2,6-diaminopyridine was recrystallized from hot toluene before to use.

The precursor complex $[\text{Cu}(\text{CH}_3\text{CN})_4](\text{ClO}_4)$ was synthesized following the literature procedure.¹⁷

Spectroscopic Measurements.

UV-vis and NMR spectra were recorded on solutions deaerated with streams of N_2 or Ar gas. 1D- and 2D-NMR spectra were recorded on deuterated solution of the complexes (1,1,2,2-tetrachloroethane $\text{C}_2\text{Cl}_4\text{D}_2$, CD_3CN , CDCl_3) at 300 K on a Bruker Avance 400 spectrometer operating at 400.13 MHz for ^1H , 100.61 MHz for ^{13}C and 161.97 MHz for ^{31}P nucleus, and equipped with a 5 mm broadband inverse probe head incorporating a z-gradient coil. The chemical shifts (in ppm) for ^1H spectra are reported relative to TMS and calibrated with respect to the residual solvent signal. $^{31}\text{P}\{^1\text{H}\}$ spectra were calibrated with respect to the external reference H_3PO_4 10%. The number of scans in each experiment was dependent on the sample concentration. The unequivocal assignment of the proton signals of the complexes was carried out by ^1H -NMR and 2D (COSY, NOESY) experiments.

Electronic spectra were measured on a Scinco S-3100 spectrophotometer at room temperature in 1.0 cm quartz cells.

Steady-state photoluminescence properties were recorded using a Horiba Fluorolog spectrometer. The solid state emission lifetime measurements were recorded using a Nd:YAG laser from Spectra Physics (Quanta-Ray Pro230). The samples were placed in a quartz tube and irradiated with a 355 nm pump beam (fwhm = 10 ns, 10 Hz repetition rate, 2.5 mJ/pulse). The photoluminescence of the complexes was measured with a monochromator (Digikrom 240, CVI Laser Corporation) coupled to a photomultiplier tube and recorded with a 1 GHz Lecroy oscilloscope. The reaction kinetics were investigated by following the absorbance change at given wavelengths of the spectrum and incorporating those changes in the % Reaction dimensionless parameter, $\xi = I_t/I_0$. In ξ , I_0 is the emission intensity at a zero time and I_t is the emission intensity determined at an instant t of the emission decay. The fitting of mono and biexponential functions to oscillographic traces was done with routines developed in OriginPro 2015. The goodness of the fittings were based in the convergence of the Red. $\chi^2 \leq 10^{-5}$ and the Adj. $R^2 \sim 0.99995$. Deconvolutions of the emission spectra into Gaussian functions were carried out using the multipeak fitting routine of OriginPro 2015, which uses similar statistical parameters for the evaluation of the fitting goodness. In this routine, an excess of contributing Gaussians to the fitting of the spectrum results in an error message while less than the correct number of Gaussians results in unacceptable values of Red. χ^2 and Adj. R^2 .

Cyclic voltammetry experiments

The Cyclic voltammetry experiments (CV) were performed with a Bio-Analytical Systems, Basi-Epsilon electrochemical workstation. The electrolytic cell was a conventional three-compartment cell, provided with Pt working electrode, Ag/AgCl_{sat} as reference electrode and Pt as the auxiliary electrode. Measurements were performed at room temperature and N₂ atmosphere, using solutions 5×10^{-4} mol/L of the complexes and 0.10 mol/L of

tetrabutylammonium perchlorate (TBAP) as supporting electrolyte in CH₃CN as solvent. The potentials are presented as $E_{1/2}$ versus Ag/AgCl_{sat}.

Crystallography

Data for compounds **(1)**, **(3)** and **(4)** were recorded on a Bruker Kappa APEX-II diffractometer and data for compound **(2)** was recorded on a Bruker APEX-II diffractometer. An arbitrary hemisphere of data was recorded for each compound at 120(2) K with graphite-monochromated Mo-K α radiation. Data were corrected for absorption and polarization effects and analyzed for systematic absences to determine the space group. Structures were solved by intrinsic phasing methods¹⁸ and the model developed and refined routinely using least-squares analysis on all reflections.¹⁹

Except where disorder is present, all non-hydrogen atoms were refined with anisotropic atomic displacement parameters. Hydrogen atoms were included in idealized positions riding on the atom to which they are bonded. $U_{iso}(H)$ was set equal to 1.2 $U_{eq}(C)$ for methylene and aromatic H and 1.5 $U_{eq}(C)$ for methyl hydrogen atoms. Within the structure of compound **(1)** small residual electron density was observed near the pendant phosphorus atoms P2 and P4. This was modeled as partial occupancy oxygen atoms on the supposition that oxidation of these pendant phosphorus atoms had occurred. Oxygen occupancies were refined to 15% and 18%, respectively.

Elemental Analysis (EA) was performed to crystalline samples of the complexes. In some cases, EA results fall within ~2% of error, which can be ascribed to solvent molecules present in the crystals, as described in the crystallographic section.

N,N'-bis(diphenylphosphine)-2,6-diaminopyridine, PNP.

The synthesis of the ligand PNP was carried out according to the reported procedure.¹⁴ 1.00 g of 2,6-diaminopyridine (9.42 mmol) were dissolved in a mixture of 50 mL of anhydrous THF and 5.25 mL of Et₃N (18.85 mmol), and allowed to react for 3 h at room temperature under N₂ atmosphere in a three-neck reactor. The reaction was cooled to 0 °C and 3.46 mL of PPh₂Cl (18.85 mmol) were slowly added, allowing the mixture to reach room temperature and reacting for 6 h under N₂ atmosphere.

The resultant solution was vacuum filtered and roto-evaporated until a brown oil was obtained. This was dissolved in a minimum amount of CHCl₃ and precipitated with diethyl ether. Crystals of PNP were obtained as colorless needles through diethyl ether diffusion over a concentrated solution of the ligand. Yield, 65%.

¹H-NMR (CDCl₃): δ(ppm)= 7.44 (m, 8H), 7.35 (t, 13H), 6.48 (d, 2H), 5.00 (d, 2H). ¹³C NMR (CD₃Cl): δ(ppm)= 157.88, 140.06, 131.73, 129.57, 128.93, 99.47.

[Cu(PNP)₂](ClO₄), (1)

0.59 g of the precursor complex [Cu(CH₃CN)₄](ClO₄) (1.78 mmol) were dissolved in 40 mL of a mixture dichloromethane-methanol 60-40 in a three-neck reactor, under nitrogen atmosphere. Then, 1.71 g of the ligand PNP (3.58 mmol) in 40 mL of CH₂Cl₂ were slowly added dropwise and the mixture was stirred for 3 h at room temperature under N₂ atmosphere. The volume of the solution was reduced by roto-evaporation and the complex was precipitated with diethyl ether. Yield 79%. Colorless crystals of **(1)** were obtained by slow ether diffusion over a CH₂Cl₂ solution of the complex.

Anal. Calcd. for $C_{58}H_{51}ClCuN_6O_4P_4$: C, 62.26; H, 4.59; N, 7.51. Found: C, 60.84; H, 4.27; N, 7.51. 1H -NMR (CD_3CN , 300K): δ (ppm)= 7.43 (t, 1H), 7.34 (t, 4H), 7.22 (t, 8H), 7.01 (s, 8H), 6.31 (d, 2H), 6.00 (s, 2H). ^{13}C NMR (CD_3CN): δ (ppm)= (-Py) 142.0, 135.9, 131.0, (-PPh₂) 131.4 (d, $^2J_{C-P}$: 18 Hz), 131.2 (overlapped), 130.5 (s), 129.3 (broad).

[Cu₂(PNP)₂(phen)](ClO₄)₂, (2)

This complex was prepared from (1) and $[Cu(CH_3CN)_4](ClO_4)$ as precursors. To 0.56 g of the complex $[Cu(CH_3CN)_4](ClO_4)$ (1.71 mmol) dissolved in a mixture of dichloromethane-methanol 60-40 in a three-neck reactor, were added 0.31 g of phen (1.71 mmol) dissolved in 40 mL of CH_2Cl_2 . Then, 1.91 g of the complex (1) (1.71 mmol) dissolved in the CH_2Cl_2 -methanol mixture were slowly added to the reactor and the reaction was kept at room temperature with a N_2 stream for 6 h.

An orange oil was obtained after evaporation of the solvents at reduced pressure. The oil was precipitated with diethyl ether to produce a yellow powder. Yellow crystals were obtained by slow ether diffusion over a concentrated solution of the complex in CH_2Cl_2 -methanol as solvent. Yield, 83%.

Anal. Calcd. for $C_{70}H_{59}Cl_2Cu_2N_8O_8P_4$: C, 57.50; H, 4.07; N, 7.66. Found: C, 57.20; H, 3.99; N, 7.67. 1H -NMR ($C_2Cl_4D_2$, 300K): δ (ppm)= 9.00 (d, 1H), 8.77 (d, 1H), 8.27 (s, 1H), 8.11 (dd, 1H), 7.96 (s, 2H), 7.66 (s, 3H), 7.38 – 7.25 (m, 5H), 7.25 (s, 1H), 7.16 (m, 6H), 7.07 (t, 2H), 6.97 (t, 3H), 6.74 (d, 2H), 6.63 (d, 2H), 6.29 (d, 1H), 5.94 (d, 1H), 4.91 (s, 1H). ^{13}C NMR ($C_2D_2Cl_4$): δ (ppm)= (-Py, phen) 157.9, 154.1, 150.7, 150.1, 143.8, 142.4, 139.1, 106.4, 101.5, (-PPh₂) 134.1, 133.8, 133.5, 133.3, 133.2, 133.1, 132.5, 131.7, 131.4, 131.1, 130.8, 130.4, 129.9, 129.6, 129.3, 128.5.

[Cu(PNP)(PPh₃)](ClO₄), (3)

0.53 g of the ligand PNP (1.11 mmol) dissolved in CH₂Cl₂ were slowly added to 0.362 g of the complex [Cu(CH₃CN)₄](ClO₄) (1.11 mmol) dissolved in 40 mL of a mixture CH₂Cl₂-methanol 60-40, contained in a three-neck reactor under N₂ atmosphere. After 30 min, 0.29 g of PPh₃ (1.11 mmol) in CH₂Cl₂ were added to the reactor and the reaction was kept under N₂ atmosphere for 3 h. The volume of the solution was reduced by roto-evaporation and diethyl ether was used to precipitate the complex as a white powder. Yield, 76%. Colorless crystals were obtained by slow ether diffusion over a CH₂Cl₂ solution of the complex.

Anal. Calcd. for: C₄₇H₄₀ClCuN₃O₄P₃ : C, 62.53; H, 4.47; N, 4.65. Found: C, 63.64; H, 4.53; N, 4.68. ¹H-NMR (C₂Cl₄D₂, 300K): δ(ppm)= 7.57 (t, 1H), 7.33 (t, 8H), 7.18 (m, 21H), 7.06 (t, 6H), 6.50 (d, 2H), 5.95 (d, 2H). ¹³C NMR (C₂D₂Cl₄): δ(ppm)= (-Py) 155.1, 143.1, 133.9, (-PPh₂, PPh₃) 133.6, 133.5, 131.5, 131.4, 130.7, 130.4, 129.1, 102.2.

[Cu(PNP)(dmp)](ClO₄), (4)

Two methods were used to prepare complex (4): The first (Scheme I), was by direct addition of complex (1) to a CH₂Cl₂ solution containing [Cu^I(CH₃CN)₄](ClO₄) and dmp in a ratio 1:1. After purification on a chromatographic column, a considerable amount of oxidized product was retained by the alumina. The yield of (4) was lower than 40%.

As a second method, in a three-neck reactor were dissolved 0.1349 g (0.41mmol) of the precursor [Cu^I(CH₃CN)₄](ClO₄) with 30 mL of CH₂Cl₂ under N₂ atmosphere. Then, 0.4327g of PPh₃ (1.65 mmol) were slowly added to the reactor and the mixture was kept under N₂ for 2 h. A white solid was obtained after roto-evaporation, yielding the complex [Cu^I(PPh₃)₄](ClO₄). The

tetraphosphine complex was dissolved in 30 mL of CH₂Cl₂ and a solution containing 0.1969 g (0.41 mmol) of the ligand PNP was added. After 2 h, the solution was roto-evaporated and the resulting white solid was washed with diethyl ether in a Soxhlet system to remove uncoordinated phosphine. After dissolution of the solid in CH₂Cl₂, 0.085 g of a neocuproine (0.41 mmol) solution were slowly added to the reactor and the yellow solution was stirred for 2 h under N₂. An orange oil was isolated after roto-evaporation. Several washes with diethyl ether to remove the free phosphine which was displaced by the ligand dmp, resulted in the precipitation of the complex [Cu(PNP)(dmp)](ClO₄). Yield: 73%.

Anal. Calcd. for C₄₃H₃₇ClCuN₅O₄P₂: C, 60.85; H, 4.39; N, 8.25. Found: C, 61.23; H, 4.35; N, 8.35. ¹H-NMR (C₂Cl₄D₂, 300K): δ(ppm)= 8.37 (d, 2H), 7.90 (s, 2H), 7.65 (2, 2H), 7.54 (t, 1H), 7.22 (t, 4H), 7.09 (t, 8H), 6.97 (d, 8H), 6.82 (d, 2H), 6.08 (s, 2H), 2.39 (s, 6H). ¹³C NMR (C₂D₂Cl₄): δ(ppm)= (-Py, dmp) 159.8, 142.1, 128.0, 138.6, 136.5, 136.4, 129.7, 126.6, 126.1, (-PPh₂) 131.2 (d, ²J_{C-P}: 19.5 Hz), 131.0 (s), 129.3 (overlapped), 129.2 (d, ³J_{C-P}: 8.4Hz), (-CH₃) 26.8.

RESULTS AND DISCUSSION

The geometry imposed by the Cu(I) atom allows the coordination of two molecules of PNP acting as bicoordinating ligands instead of the pincer-like tri-coordination. Consequently, there are two donor atoms that are able to bind a second copper atom. The complex thus formed, $[\text{Cu}(\text{PNP})_2]^+$ (**1**), can be used as a precursor for new bimetallic complexes. On the basis of this proposal, the bimetallic complex $[\text{Cu}^{\text{I}}_2(\text{PNP})_2(\text{phen})]^{2+}$ (**2**) was prepared by mixing equimolar amounts of $[\text{Cu}(\text{PNP})_2]^+$ and $[\text{Cu}(\text{phen})(\text{CH}_3\text{CN})_2]^+$, Scheme I.

Under similar experimental conditions used for the preparation of (**2**), the syntheses of other two bimetallic compounds were attempted. One derived from triphenylphosphine ($[\text{Cu}^{\text{I}}_2(\text{PNP})_2(\text{PPh}_3)_2]^{2+}$) and another derived from neocuproine ($[\text{Cu}^{\text{I}}_2(\text{PNP})_2(\text{dmp})]^{2+}$). However, the addition of equimolar amounts of $[\text{Cu}(\text{PPh}_3)_2(\text{CH}_3\text{CN})_2]^+$ to the solution containing complex (**1**) leads to the rearrangement of both complexes and the formation of two equivalents of a new monometallic complex, $[\text{Cu}^{\text{I}}(\text{PNP})(\text{PPh}_3)]^+$ (**3**), Scheme I. This is most likely due to the steric hindrance produced by the triphenylphosphine ligand, which is bulky enough to prevent the coordination of two PPh_3 to the same copper atom. Complex (**3**) has an unusual geometry with PNP tricoordinated as a pincer ligand. This complex can also be synthesized in higher yields mixing Cu(I), PNP and PPh_3 , in a ratio 1:1:1, as described in the experimental section.

The preparation of the neocuproine binuclear complex was attempted in a reaction where $[\text{Cu}(\text{PNP})_2]^+$ and $[\text{Cu}(\text{dmp})(\text{CH}_3\text{CN})_2]^+$ were mixed in stoichiometric amounts. The reaction yield the heteroleptic complex $[\text{Cu}^{\text{I}}(\text{PNP})(\text{dmp})]^+$ (**4**), and oxidation products which were not studied in this work. Despite the fact that phen and dmp have similar structures, models suggest that the steric hindrance caused by the 2,9-dimethyl substituents in dmp causes steric congestion with the diphenylphosphine groups that impedes the formation of a bimetallic species. The yields

in the synthesis of complex **(4)** can also be improved by the separate method described in the experimental section.

The set of complexes of PNP and secondary ligands such as PPh₃ or dmp obtained in this work reveal the versatility of the PNP ligand when it is coordinated to Cu(I). Indeed, it is able to function in a pincer-fashion, as a bicoordinating ligand and as a tricoordinating ligand to form bimetallic species.

Structural characterization in solution and solid phase.

Crystallographic structures.

The crystal structures **(1)** - **(4)** are analyzed in terms of the geometrical parameter, τ_4 , for four-coordinated complexes proposed by Yang *et al.*,²⁰ which uses the bond angles of the primary coordination sphere of the metal atom to establish a numerical value related to geometry. The values of τ_4 will range from 1.00 for a perfect tetrahedral geometry, to zero for a perfect square planar geometry. Intermediate structures, including trigonal pyramidal and “seesaw”, fall within the range 0.00 to 1.00.

The complex [Cu(PNP)₂](ClO₄) **(1)** crystallizes as yellow block-like crystals. There are four molecules of the copper cation and associated perchlorate anion in the unit cell of the monoclinic space group P2₁/n. The complex consists of a copper coordinated by one phosphorous and the pyridine nitrogen of each PNP ligand, leaving one pendant uncoordinated phosphorus on each PNP ligand, Fig. 1. The copper atom has a τ_4 value of 0.72, indicative of a seesaw geometry. A small, yet significant amount, of residual electron density located about 1.4 Å from both pendant phosphorus atoms was observed in a difference Fourier map. Given the propensity for

phosphines to form phosphine oxides, it is not unreasonable that a similar process occurred here and that there is a small percentage of phosphine oxide present in the lattice.

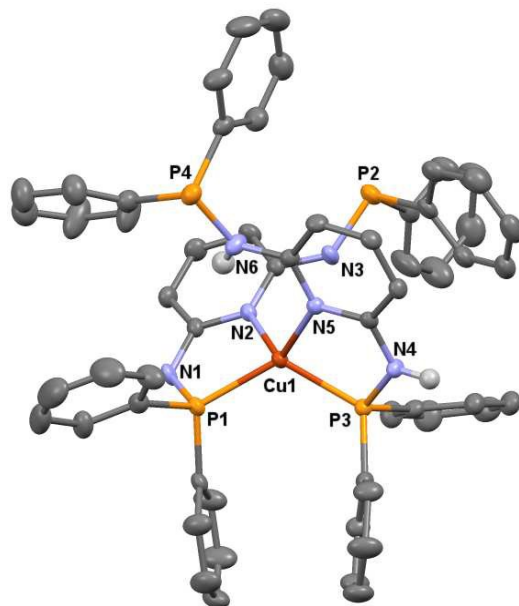


Figure 1. Molecular structure of $[\text{Cu}(\text{PNP})_2](\text{ClO}_4)$, (1).

The bond distances and angles between Cu and the coordinating atoms in both PNP ligands are similar: The distance from Cu(1) to N(2) and N(5) are almost identical, 2.069 and 2.059 Å, respectively. The same for Cu(1)-P(1)/P(3), with distances of 2.209 and 2.222 Å. Also, angles formed in the coordinative environment of the copper atom are similar, P(1)-Cu(1)-(N2) = 85.95° and P(3)-Cu(1)-N(5) = 86.07°.

The synthesis of the complex $[\text{Cu}(\text{PNP})_2]^+$ with iodide as counterion (the same PNP ligand) has been already reported by Pan *et al.*¹² from the reaction of copper(I) iodide with PNP in a molar ratio 1:2. While crystals were obtained, the quality of the crystals prevented these authors from making a full refinement of the structure. In our treatment of $[\text{Cu}(\text{PNP})_2]\text{ClO}_4$ crystals of a sufficient quality were obtained for a full refinement of the structure.

Compound	(1)	(2)	(3)	(4)
Empirical formula	C ₅₈ H ₅₀ ClCuN ₆ O _{4.34} P ₄	C ₇₁ H ₆₁ Cl ₃ Cu ₂ N ₈ O _{8.50} P ₄	C ₄₇ H ₄₀ ClCuN ₃ O ₄ P ₃	C ₄₃ H ₃₆ ClCuN ₅ O ₄ P ₂
Formula weight (g/mol)	1123.35	1519.58	902.72	847.70
Temperature (K)	120(2)	120 (2)	120(2)	120(2)
Cryst. Syst., space group.	Monoclinic, <i>P2_{1/n}</i>	Triclinic, <i>P-1</i>	Monoclinic, <i>P2_{1/n}</i>	Triclinic, <i>P-1</i>
Unit cell dim. (Å, deg)				
<i>a</i> (Å)	19.6651(16)	12.8814(18)	10.4216(9)	9.5788(11)
<i>b</i> (Å)	12.1590(11)	14.442(2)	30.083(3)	13.3745(16)
<i>c</i> (Å)	22.774(2)	22.538(3)	13.3873(11)	17.068(2)
α , deg.	90°	107.055(2)°	90°	105.687(3)°
β , deg.	104.059(2)°	94.260(2)°	90.832(2)°	93.029(3)°
γ , deg.	90°	111.323(2)°	90°	101.325(3)°
volume (Å ³)	5282.4(8)	3656.2(9)	4196.6(6)	2051.1(4)
Z	4	2	4	2
Calculated density (g/cm ³)	1.413	1.380	1.429	1.373
Absorption coeff. (μ) (mm ⁻¹)	0.640	0.838	0.747	0.724
<i>F</i> (000)	2323	1560	1864	874
crystal size (mm ³)	0.22 × 0.15 × 0.08	0.29 × 0.26 × 0.14	0.28 × 0.26 × 0.08	0.26 × 0.18 × 0.07
θ range (deg)	1.229° to 26.394°	1.568° to 28.305°	1.665° to 26.482°	1.621° to 26.516°
Index ranges	-24 ≤ <i>h</i> ≤ 24, -15 ≤ <i>k</i> ≤ 15, -28 ≤ <i>l</i> ≤ 28	-17 ≤ <i>h</i> ≤ 16, -19 ≤ <i>k</i> ≤ 19, -26 ≤ <i>l</i> ≤ 30	-13 ≤ <i>h</i> ≤ 13, -37 ≤ <i>k</i> ≤ 37, -16 ≤ <i>l</i> ≤ 16	-12 ≤ <i>h</i> ≤ 10, -16 ≤ <i>k</i> ≤ 16, -21 ≤ <i>l</i> ≤ 21
Reflns. collected/unique	63333	49882	45776	31677
Independent reflections	10809 [Rint = 0.0558]	18003 [Rint = 0.0255]	8620 [Rint = 0.0640]	8460 [Rint = 0.0669]
Completeness to θ (%)	100%	100 %	100 %	100%
Absorption correction	Numerical	Numerical	Numerical	Numerical
Max and min transmn.	1.0000 and 0.9064	0.9830 and 0.8902	1.0000 and 0.9082	0.9795 and 0.9433
Data/restraints/parameters	10809 / 0 / 677	18003 / 14 / 907	8620 / 0 / 532	8460 / 0 / 505
GOF on F ²	1.022	1.027	1.013	1.044
Final R indices [<i>I</i> > 2 σ (<i>I</i>)]	R ₁ = 0.0395, wR ₂ = 0.0906	R ₁ = 0.0414, wR ₂ = 0.1142	R ₁ = 0.0369, wR ₂ = 0.0753	R ₁ = 0.0522, wR ₂ = 0.1286
R indices (all data)	R ₁ = 0.0617, wR ₂ = 0.1010	R ₁ = 0.0538, wR ₂ = 0.1220	R ₁ = 0.0624, wR ₂ = 0.0849	R ₁ = 0.0887, wR ₂ = 0.1471
Largest diff peak and hole (e/Å ³)	0.602 and -0.391	2.318 and -0.770	0.448 and -0.514	0.647 and -0.951

Table 1 : Crystallographic data and refinement.

Aside from the parameters communicated in Table I, our observations and those of Pan *et al.* are in agreement. According to these results, $[\text{Cu}(\text{PNP})_2]\text{I}$ crystallizes in the same space group (monoclinic $\text{P}2_1/\text{n}$), where the copper cation is tetracoordinated in a tetrahedral geometry by the pyridine nitrogen and one $-\text{PPh}_2$ of each PNP ligand, leaving two pendant diphenylphosphine groups in the molecule. In addition, the number of molecules ($Z=4$) in the unit cell and the cell parameters of both structures are very similar (Table 1), which may indicate that the solid structures of both the cation are closely related in the perchlorate and iodide complexes.

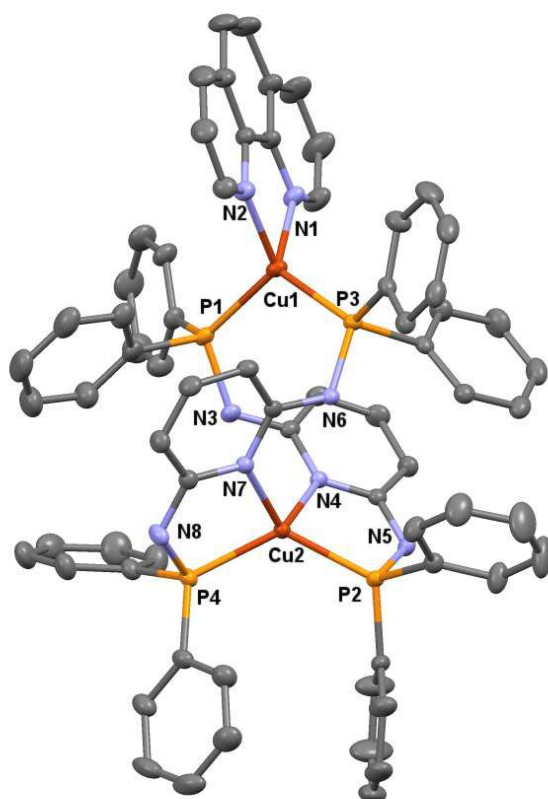


Figure 2. Molecular structure of $[\text{Cu}_2(\text{PNP})_2(\text{phen})](\text{ClO}_4)_2$, (**2**).

The complex (**2**) crystallizes as pale yellow block-like crystals from a dichloromethane/ethanol solution. There is one molecule of the bimetallic complex with two Cu(I) cations, two associated perchlorate anions, one half dichloromethane and five molecules of ethanol within the asymmetric unit of the triclinic space group P-1. This copper complex, Fig. 2, consists of two copper centers with distorted tetrahedral coordination geometry, where Cu(1) is coordinated by the two N atoms of a phenanthroline ligand (Cu(1)- N1/N2=2.078(2)/2.091(2) Å) and the terminal phosphorus atoms of two PNP ligands (Cu(1)-P1/P3=2.2686(7)/2.2481(6) Å). The τ_4 value is 0.82 for this copper, indicating a slightly distorted tetrahedral environment. The second copper is coordinated by the two pyridine nitrogen atoms (Cu(2)-N4/N7=2.077(2)/2.078(2) Å) and the two remaining phosphorus atoms of the PNP ligands (Cu(2)-P2/P4=2.2135(7)/2.2142(8) Å). The geometry of Cu(2) deviates more from an ideal tetrahedron and is close to a seesaw geometry, $\tau_4 = 0.73$. In addition, the wrapping of the PNP ligands around the copper atoms determines the helical nature of the complex, where both M and P enantiomers crystallize as a racemic mixture in the unit cell, Fig. 3.

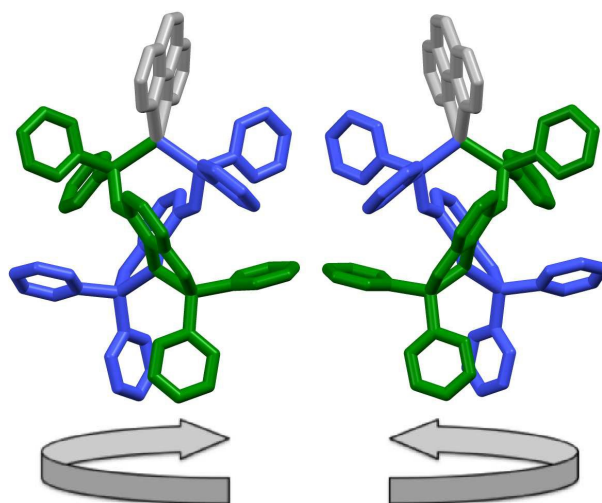


Figure 3. Molecular structure of enantiomers *M*-(**2**) (left) and *P*-(**2**) (right). PNP ligands are colored to highlight the helicity of the enantiomers.

The preference of the copper (I) atom in adopting a tetrahedral geometry, and the flexibility of PNP when acting as bicoordinating ligand, are factors that favor helicity in the bimetallic complex. A third feature, a $\pi\pi$ -interaction between the pyridine ring of one PNP and the phenyl ring of the another PNP also contributes to the formation of this bimetallic helicate. These $\pi\pi$ -interactions are characterized by centroid to centroid distances of 3.882 and 3.695 Å. Previously, we have observed²¹ that the folding of the ligands upon coordination to yield a helicate complex allows the establishment of $\pi\pi$ -interactions capable of stabilizing the helicate conformation. These are not feasible when the conformation is that of a mesocate complex. This complex is added to the few examples of Cu(I) bimetallic helicates derived of pincer ligands.^{22, 23}

Complex **(3)** crystallizes as yellow, tablet-like crystals. There are four molecules of the complex and associated perchlorate anions in the unit cell of the centrosymmetric, monoclinic space group $P2_1/n$. The copper center is coordinated in a four-coordinate “butterfly” or seesaw fashion by the nitrogen and phosphorus atoms of the PNP pincer ligand and the phosphorus of a triphenylphosphine ligand, Fig. 4.

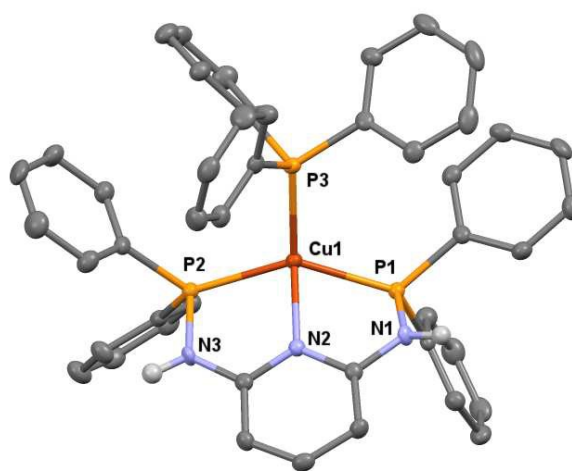
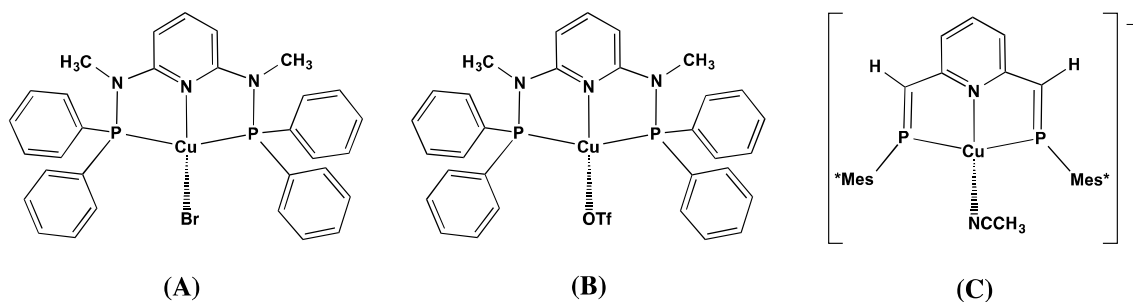


Figure 4. Molecular structure of $[\text{Cu}(\text{PNP})(\text{PPh}_3)](\text{ClO}_4)$, **(3)**.

Inspection of the bond angles about the Cu center shows the highly distorted nature of the coordination geometry. The τ_4 calculation yields a value of 0.67, which is intermediate between square planar ($\tau_4 = 0$) and tetrahedral ($\tau_4 = 1$). Presumably, the steric bulk of the triphenylphosphine ligand enforces such distortions. There is some degree of twisting involved in the PNP ligand coordination. The sum of the angles involving N2-Cu1-P1/2 is 162.78° while the P1-Cu-P2 bond angle is only $139.85(2)^\circ$. The complex forms one-dimensional H-bonded chains in the solid state. The chains are propagated by hydrogen bonds from the amine nitrogen, N1 to a perchlorate oxygen (O1) and from the amine, N3, to a perchlorate oxygen (O2') related by the crystallographic *c*-glide plane.

Recently, Richeson *et al.*¹⁰ reported two neutral copper-pincer complexes, [2,6-{Ph₂PNMe}₂(NC₅H₃)]CuBr (A, Scheme II) and [2,6-{Ph₂PNMe}₂(NC₅H₃)]CuOTf (B, Scheme II) ([2,6-{Ph₂PNMe}₂(NC₅H₃)] = N,N'-bis(diphenylphosphine)-2,6-di(methylamino)pyridine and OTF (= OSO₂CF₃), where the pincer ligand is tri-coordinated at the copper center in a similar manner to **(3)**, with bromine or OTF as the fourth ligand in a geometry described as trigonal pyramidal ($\tau_4 = 0.78$ for A and $\tau_4 = 0.75$ for B). Most of the bond distances between the pincer fragment and the copper atom in A and B are smaller than in **(3)**. For complex A, Cu-P distances are 2.2245 and 2.2386 Å and the Cu-N_{py} distance is 2.1230 Å, while in complex B the Cu-P distances are 2.2264 and 2.2301 Å and the Cu-N_{py} distance is 2.0574 Å, which is the slightly shorter than that in cationic complex (Cu-N_{py} = 2.070(2) Å) **(3)**.



Scheme II

Interestingly, the Cu-PNP fragment in **(3)** matches closer to another complex reported by Hayashi *et al.*,⁹ [Cu(PNP)(CH₃CN)]PF₆, (C, Scheme II) where the PNP is a 2,6-Bis-(phosphaethenyl)pyridine ligand with a 2,4,6-tri-*t*-butylphenyl substituent (Mes*) at each phosphorus atom. Only small differences in the bond distances for the Cu-PNP fragments of both complexes are found: For complex C, Cu-P distances are 2.313(2) and 2.303(1) Å and Cu-N_{py} distance is 2.071(4) Å. The P-Cu-P angle is slightly larger in C (141.43°), ascribed to the smaller steric hindrance of the MeCN ligand compared to the bulky PPh₃ which forces to the Cu atom to move away from the P-N_{py}-P plane in **(3)**. In addition, the phosphaethenyl complex has the same τ_4 value that **(3)** ($\tau_4 = 0.67$), both complexes having a seesaw geometry.²⁴

Despite the similarity between the PNP ligands in A, B and **(3)** (a methyl substituent instead H at the non-coordinating amines), bond distances, angles and geometry around the copper atom are almost identical to the complex C, where the PNP ligand is substantially different. On this basis, it is tempting to relate this to the cationic nature of complexes [Cu(PNP)(PPh₃)]⁺ and C, in contrast to the neutral complexes A and B.

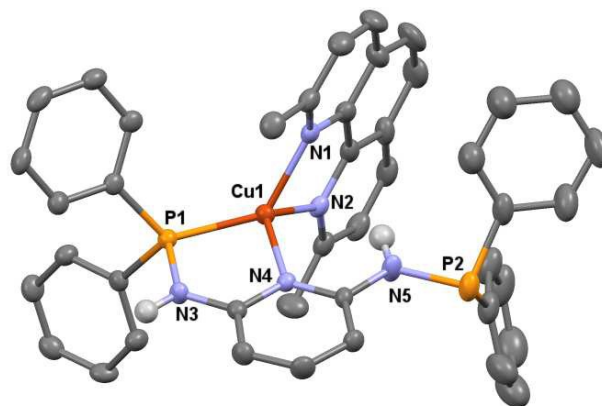


Figure 5. Molecular structure of $[\text{Cu}(\text{PNP})(\text{dmp})](\text{ClO}_4)$, (**4**).

The complex (**4**) crystallizes as yellow block-like crystals from an ethanol solution. There are two molecules of the Cu cation and associated perchlorate anion in the unit cell of the centrosymmetric triclinic space group P-1. The Cu is coordinated in a distorted tetrahedral fashion by the two nitrogen atoms of the dmp ligand and the pyridine nitrogen and one phosphorus of the PNP ligand, Fig. 5. The remaining phosphorus of the PNP ligand is not coordinated. The τ_4 value for the Cu center is 0.70, indicative of a seesaw geometry. The Cu-N_{dmp} distances are all similar (2.05 – 2.08 Å) and the Cu-P bond distance is 2.1876(10) Å. The amide N3, forms a hydrogen bond to one perchlorate oxygen, while the amide N5 is oriented towards the five-membered chelate ring formed by the phenanthroline and the copper.

NMR characterization and fluxional behavior

A number of NMR experiments were performed to assess both structural and redox stability of the copper complexes in solution. In general, well defined proton signals are observed for all the compounds, indicating that no oxidation to Cu(II) occurs under the experimental conditions. VT-NMR experiments were carried out for complexes **(1)** and **(4)**, where there is the possibility of fluxionality based on their crystal structures and other information.

The 1-D (^1H , ^{31}P) and 2-D NMR spectra of the homoleptic complex **(1)** were recorded in deuterated acetonitrile as solvent (Figs. S1, S2). In ^{31}P NMR, the observation of only one signal of coordinated PNP contrasts with expectations from the crystal structure of this complex, where only one diphenylphosphine moiety is coordinated to the copper, for each PNP ligand. No significant ^{31}P signal corresponding to P(V) from phosphine oxide was detected around 20.3 ppm.

The half-width of the unique broad signal centered around 28.0 ppm to phosphorus ($\Delta\nu_{1/2}=213.5$ Hz at 300K) is considerably broader than the free PNP ligand ($\Delta\nu_{1/2}=5.7$ Hz), suggesting a fluxional behavior in solution, where both phosphine moieties of each PNP ligand are alternating for the copper coordination, at rates comparable to the detection rate of the instrument.

In order to determine energetic parameters involved in such an intramolecular exchange, ^{31}P VT-NMR experiments for **(1)** were performed in CD_3CN in the range 228-256 K, Fig. 6. At temperatures below 240 K, the ^{31}P signal splits in two broad singlets, corresponding to two coordinated and two uncoordinated phosphorus atoms, while complete coalescence occurs at $T_c \approx 244$ K. Rate constants for the phosphorus exchange were obtained through the line-shape analysis by fitting to Bloch derived equations, Fig. 6.

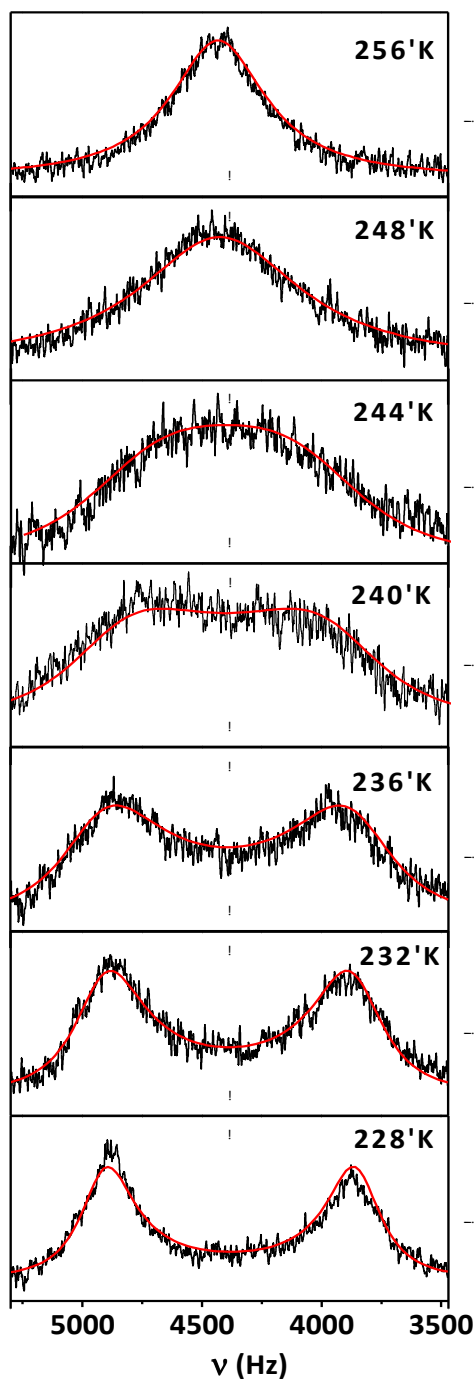


Figure 6. ^{31}P VT-NMR of **(1)** in CD_3CN at temperature range 228-256 K. The simulated bands by lineshape analysis are represented by red curves. Rates constants (s^{-1}): 1.76×10^3 , 2.28×10^3 , 3.33×10^3 , 4.78×10^3 , 5.78×10^3 , 1.52×10^4 , 2.41×10^4 at 228 K, 232 K, 236 K, 240 K, 244 K, 248 K and 256 K, respectively.

An activation energy value of $E_a=47.42$ kJ/mol was determined from an Arrhenius plot ($\ln k$ vs $1/T$) and the activation parameters were derived from an Eyring plot are: $\Delta H^\ddagger=45.42$ kJ/mol, $\Delta S^\ddagger=17.40$ J/K mol, $\Delta G^\ddagger=40.23$ kJ/mol (calculated at 298K), Fig. S3. Activation energy values can be compared with those of complexes undergoing a similar intramolecular exchange. For instance, Abel *et al.*²⁵ reported the fluxional behavior of terpyridine when is acting as a bicoordinating ligand in the square planar complexes $[M(C_6F_5)_2(terpy)]$, namely $E_a=75.7$, $\Delta H^\ddagger=72.8$ kJ/mol, $\Delta S^\ddagger=5.8$ J/K mol, $\Delta G^\ddagger=71.0$ kJ/mol for $M=Pd$ and $E_a=77.0$, $\Delta H^\ddagger=74.1$ kJ/mol, $\Delta S^\ddagger=10.8$ J/K mol, $\Delta G^\ddagger=70.9$ kJ/mol for $M=Pt$.

In the Pd and Pt complexes, the alternating coordination of the non-central pyridine rings in *terpy* must occur in a square-planar geometry, where steric effects can further influence the dynamics. A lower activation energy value for the fluxional process of **(1)** in tetrahedral geometry can be expected as a result of the lability of Cu(I) given the lack of crystal field stabilization energy in the d^{10} configuration.²⁶

A smaller activation energy value ($E_a=33$ kJ/mol in THF- d_8) accounting for a more rapid intramolecular arrangement was reported by Petrovic *et al.*¹¹ for the similar Cu(I)-pincer complex, $[(TL^{tBu})CuBr]$, where $TL^{tBu}=2,6$ -bis[(1,3-di-tert-butylimidazolin-2-imino)methyl]pyridine. This complex crystallizes with the ligand coordinated in a chelating fashion $[(TL^{tBu}-\kappa N^1:\kappa N^2)CuBr]$, which leaves the copper(I) atom tri-coordinated in a trigonal-planar geometry, whereas in solution the coordinated and uncoordinated arms of the ligand can be differentiated by NMR at temperatures below $T_c=176$ K.

According to its crystal structure, complex **(2)** corresponds to a bimetallic complex with both copper atoms in different chemical environments, resulting in the loss of symmetry of the PNP ligand and a more complex pattern of proton signals in the NMR spectra. For complex **(2)**, the numbering of the protons of the PNP and phen ligands is shown in Fig. S4 (NMR spectra in Figs. S5-S8 and assignments in Table S1). For the phenanthroline coordinated to Cu(1) (Fig. 2), the ^1H signals are those expected for a symmetrically coordinated phenanthroline ligand suggesting that the compound in solution has a symmetry axis crossing both copper atoms and bisecting the phenanthroline ligand.

The shielding effect of the phenanthroline ligand shifts to higher field the protons of the $-\text{PPh}_2$ groups coordinated to Cu(1), where they appear as a double set of well-defined signals, stemming from the different chemical environments perceived by the protons pointing to the phen ligand on each phenyl ring. By contrast, the protons of the $-\text{PPh}_2$ groups coordinate to Cu(2) appear at lower field and the signals have lower resolution, due to lower steric hindrance and a greater possibility that molecular motions of the phenyl rings, result in broader signals.

From the ^1H -NMR and NOESY spectra, it is possible to conclude that this complex retains its helical nature in solution and its conformation must be very similar to that observed in the crystal structure. For example, the diastereotopic behavior of protons on both phenyl rings in the couple of phosphines coordinated to Cu(1) (6.5 -7.0 ppm, Fig. S5) is indicative of helicity of the complex in solution phase. Also, a NOESY interaction between H3' on the pyridine rings (5.94 ppm) and H2, H9 on the phenanthroline ligand (9.0 ppm) is only possible when the complex has a folding way as that observed in its crystal structure (Fig. S8). In fact, according to the crystal structure, the distance between both interacting protons is $\sim 2.5 \text{ \AA}$, which is in the range of distances that NOESY interactions are detected.

In the ^{31}P spectrum of the complex **(2)** in $\text{C}_2\text{Cl}_4\text{D}_2$ (Fig. S7), two singlet signals at $\delta=42.14$ ppm ($\Delta\nu_{1/2}=73.76$ Hz) and $\delta=31.20$ ppm ($\Delta\nu_{1/2}=57.53$ Hz), are observed in agreement with the symmetry of the molecule in solution where both $-\text{PPh}_2$ groups coordinated to Cu(1) are equivalent to each other as are the two phosphine groups coordinated to Cu(2). No significant variation associated to fluxionality of the complex was observed by recording the ^{31}P spectrum at different temperatures.

The monometallic and heteroleptic nature in solution of the complex **(3)** was unequivocally confirmed by the concerted use of 1-D and 2-D NMR techniques using $\text{C}_2\text{Cl}_4\text{D}_2$ as solvent (Figs. S9-S10). The integration of the proton signals agrees with one PNP and one PPh_3 ligand, both shifted respect to the free ligands. The ^{31}P spectrum consist of two phosphorus signals coupled to each other: A doublet at $\delta=40.40$ ppm, corresponding to two P atoms of PNP ligand, and a triplet at $\delta=3.58$ ppm corresponding to one P atom of the PPh_3 ligand. Narrow signals in the ^{31}P spectrum recorded at room temperature agree with no fluxional behavior in solution.

The ^1H -NMR spectrum of **(4)** in $\text{C}_2\text{Cl}_4\text{D}_2$ (Fig. S11) shows the pattern of signals of the dmp and PNP ligands, both shifted to low field relative to the free ligands. In solution of deuterated acetonitrile, an intramolecular exchange process similar to the described for the complex **(1)** is expected because, as observed in the crystal structure of **(4)** (Fig. 6), one diphenylphosphine group in PNP is not coordinated to the copper atom.

The ^{31}P spectrum of **(4)** at 300 K consists of an unique broad signal at 23.2 ppm ($\Delta\nu_{1/2}=135.9$ Hz) in accord with an intramolecular exchange process. However, in VT-NMR experiments performed between 280 and 224K (Fig. S12), the splitting of the ^{31}P signal was not observed.

Furthermore, the peak width varies only slightly in the range of temperatures measured, $\Delta\nu_{1/2}$ =136 Hz and 177 Hz at 224 and 280K, respectively. At the lower temperatures (224 and 228K), a shoulder is observed at high field with respect to the main ^{31}P peak, suggesting that at temperatures below 224K both phosphorus signals might be resolved and the intramolecular exchange would occur at rates lower than the detection rate of the instrument.²⁷

From the simplest analysis of the fluxional behavior in **(4)** and **(1)**, it can be concluded that the phosphine moieties in **(4)** are exchanging at rates higher than those in the homoleptic complex **(1)**. However, in complex **(1)** there are four phosphorus atoms exchanging for the copper coordination, whereas in complex **(4)** only two phosphines are alternating the coordination. Taking this into account, it is not surprising that the activation energy for the fluxional process in **(4)** should be smaller than the value of **(1)**.

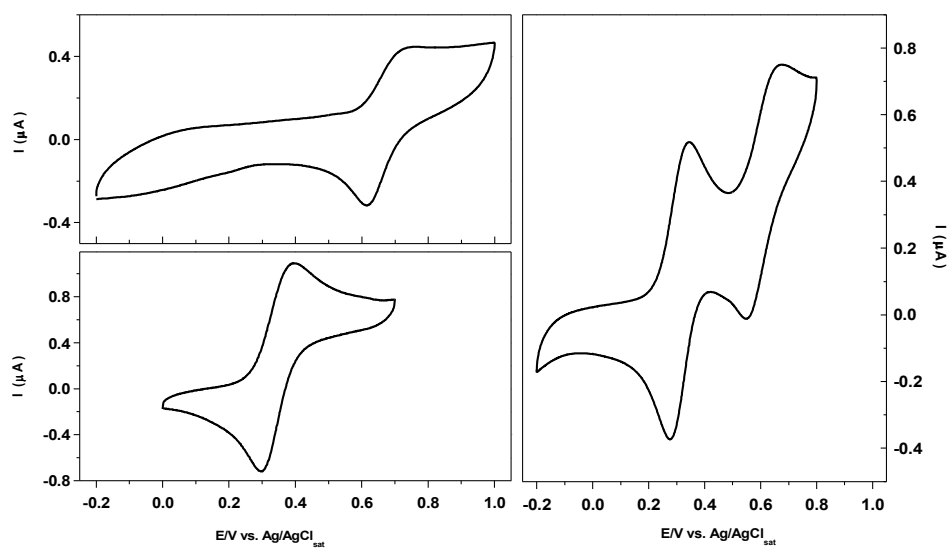
Redox behavior of Cu(II)/Cu(I) couples.

The redox behavior of the set of complexes was investigated by cyclic voltammetry, given the dependence of the coordination geometry around the copper atom, on the potentials of the $\text{Cu}^{\text{II}}/\text{Cu}^{\text{I}}$ couples. A general experimental observation is that oxidation of Cu(I) is difficult when complexes are bearing bulky ligands, considering the change of geometry upon oxidation (flattening of coordinative environment), shifting the oxidation potentials toward more positive values. Conversely, Cu(I) centers can be more facile oxidized when complexes have extended aromatic ligands, for example phen or dmp ligands in comparison to the phosphine moieties of PNP. Cyclic voltammetry experiments were carried out with CH_3CN solutions containing 5×10^{-4} M of the complexes and 0.10 M of the TBAP supporting electrolyte. An $\text{Ag}/\text{AgCl}_{\text{sat}}$ electrode was used as the reference electrode.

Table 2. Cyclic voltammetry results for (1)-(4) in CH₃CN and Ag/AgCl_{sat} as reference.

Complex	E _{ap} (mV)	E _{cp} (mV)	E _{1/2} (mV)	ΔE _p (mV)
(1)	758	615	687	143
(2)	Cu(1) 345	Cu(1) 276	310	69
	Cu(2) 680	Cu(2) 548	614	138
(3)	682	576	629	106
(4)	390	301	345	89

Despite the relationship between coordination geometry and oxidation state for copper complexes, a clear relationship between the coordination environment of the copper atom as deduced from the comparison of the τ_4 values and the potential, E_{ap}, at which oxidation occurs, was not found, Table 2.

**Figure 7.** Cyclic voltammetry of complexes: a) (1), b) (4) and c) (2), at 5×10^{-4} M of complex in CH₃CN and scan rates of 50 mV/s, Ag/AgCl_{sat} as reference.

The half wave potential of the couple $\text{Cu}^{\text{II}}/\text{Cu}^{\text{I}}$, $E_{1/2} = 687 \text{ mV}$, of **(1)** is higher than the other complexes reported here, Fig. 7a and Table 2. In the oxidation of Cu(I) to Cu(II), steric constraints imposed by the PNP ligand prevent the change of geometry from tetrahedral to square-planar which results in the $E_{1/2}$ increase. The ΔE_p value is also the highest for this series, $\Delta E_p=143 \text{ mV}$, and the couple is therefore a quasi-reversible process, being both observations consistent with a constrained geometry change. Complex **(4)** exhibit a somehow different behavior with the $\text{Cu}^{\text{II}}/\text{Cu}^{\text{I}}$ redox couple at $E_{1/2}=345 \text{ mV}$ and $\Delta E_p=89 \text{ mV}$, Fig. 7b, corresponding to a more reversible and less geometrically constrained process compared to **(1)**. The small difference between the values of $E_{1/2}$ and ΔE_p for complex **(4)** ($E_{1/2}=345 \text{ mV}$; $\Delta E_p=89 \text{ mV}$) and **(2)** ($E_{1/2}=310 \text{ mV}$; $\Delta E_p=69 \text{ mV}$, for Cu(1)) can be explained in terms of the increased steric effect generated by the presence of $-\text{CH}_3$ groups in the dmp ligand.

Two redox $\text{Cu}^{\text{II}}/\text{Cu}^{\text{I}}$ couples, Fig. 7c, can be seen in the cyclic voltammogram of the bimetallic complex **(2)**. The first couple appears as a reversible redox process with $\Delta E_p(1)=69 \text{ mV}$ and $E_{1/2}(1)=310 \text{ mV}$, while the second couple is a quasi-reversible process with $\Delta E_p(2)=138 \text{ mV}$ and $E_{1/2}(2)=614 \text{ mV}$.

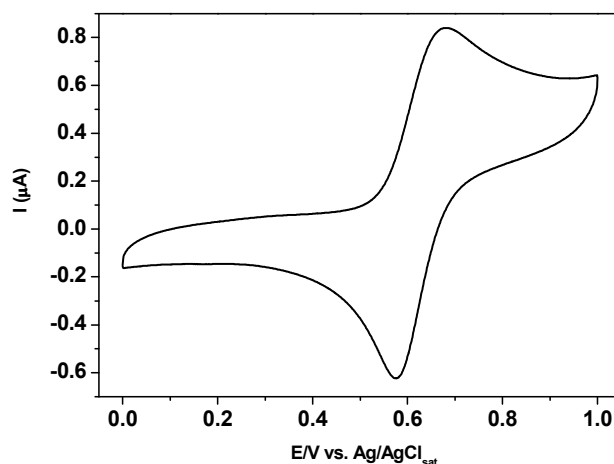


Figure 8. Cyclic voltammetry of **(3)**, $5 \times 10^{-4} \text{ M}$ in CH_3CN , scan rate 50 mV/s .

The emergence of two couples in the CV is a consequence of the copper atoms being in different coordination environments. Considering some similarities between the cyclic voltammograms of complexes **(1)** and **(4)** with the one of **(2)**, it is possible to draw a parallel between the coordination environments of the individual Cu(I) atoms in **(1)** and **(4)** and the two Cu(I) atoms in **(2)**.

For the heteroleptic monometallic complex **(3)**, a single quasi-reversible Cu^{II}/Cu^I redox couple is observed at $E_{1/2}=629$ mV and $\Delta E_p=106$ mV, Fig. 8. The Cu^{II}/Cu^I couple in this complex is more reversible than in **(1)**. It is possible to rationalize the different behavior on the basis of the τ_4 values obtained for both complexes: The τ_4 values show that the Cu atom in **(3)** has a coordination environment closer to square-planar geometry ($\tau_4=0.67$) compared to **(1)** ($\tau_4=0.72$), favoring the divalent oxidation state.

Spectroscopy of the PNP complexes

The absorption spectra of the PNP ligand and the four Cu(I) complexes are shown in Fig. 9. They exhibit absorption features in the range of 250-350 nm that are assigned to PNP-centered transitions. A comparison of the spectra of complexes **(1)** and **(3)** with the spectrum of the ligand PNP, reveal that, in addition of PNP-centered transitions, there must be overlapping absorptions due to Cu to PNP charge transfer transitions, i.e., to $MLCT_{Cu(I) \rightarrow PNP}$ excited states. Indeed, since the reduction potential of the PNP/PNP^{•-} ($E_{1/2} = -1.5$ V vs NHE) is considerable more negative than those of the L/L^{•-}, L= phen, dmp, absorptions originated in transitions to the $MLCT_{Cu(I) \rightarrow PNP}$ excited states must be considerably blue shifted, i.e., $300 \leq \lambda_{max} \leq 350$ nm, with respect to those originated in transitions to the $MLCT_{Cu(I) \rightarrow L}$ L= phen, dmp, excited states. The respective electronic transitions to $MLCT_{Cu(I) \rightarrow L}$, L= phen, dmp, excited states are clearly observed in the

spectrum of the complexes **(2)** and **(4)** as broad and less intense bands at longer wavelengths, i.e., $\lambda > 350$ nm.

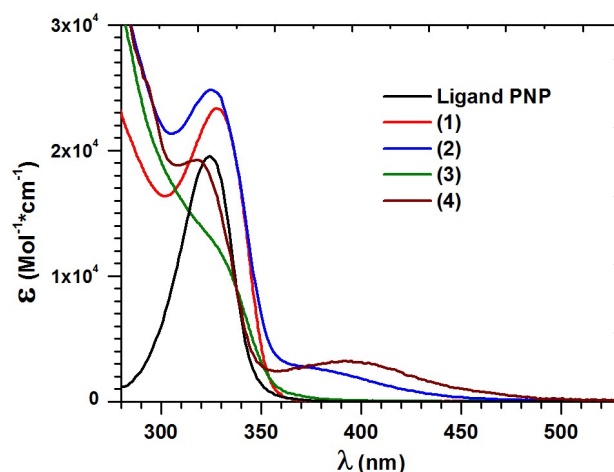


Figure 9. Absorption spectra for the ligand PNP and **(1)-(4)** complexes in CH_2Cl_2 .

The PNP ligand and the Cu(I) complexes were found to luminesce when they were irradiated in deaerated CH_3CN or CH_2Cl_2 at wavelengths of the PNP-centered transitions, i.e. $\lambda_{\text{exc}} = 330$ nm. Broad emission bands, centered at about 375-390 nm, were recorded irradiating their solutions in deaerated CH_2Cl_2 at $\lambda_{\text{exc}} = 330$ nm, Fig. 10.

The asymmetric shape of the emission bands shown in Figs. S13 - S17 suggested that they were convolutions of several emission bands. This observation was also verified de-convoluting the spectra into several Gaussians. The bands in the emission spectra of the PNP ligand and complexes **(1)** and **(3)** were resolved into three Gaussians spread over the 345 - 500 nm (20 kK - 29 kK) range. Similarities observed between the Gaussians fitting the PNP, **(1)** and **(3)** emission spectra suggest that PNP-centered electronic transitions make the major contributions to the emission spectra, Figs. S13 - S15.

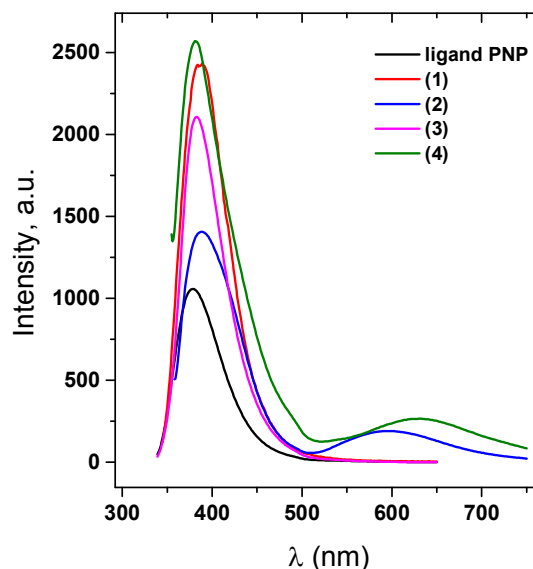


Figure 10. Emission spectra of the PNP ligand and its Cu(I) complexes in deaerated CH_2Cl_2 recorded at $\lambda_{\text{exc}} = 330$ nm.

The emissions from $\text{MLCT}_{\text{Cu(I)} \rightarrow \text{L}}$, L = phen, dmp, excited states are respectively de-convoluted by Gaussians at 617 nm (16.20 kK) and 665 nm kK (15.05), Figs. S16, S17. Three additional Gaussians are de-convoluted from the higher intensity emission band positioned at $\lambda < 517$ nm ($\tilde{\nu} > 19.4$ kK) which are in the same spectral region, 500 - 345 nm (20 - 29 kK) of those de-convoluted from the (1) and (3) spectra. However, pronounced differences between the amplitudes of the Gaussians in (1), (3) and those in (2), (4) can be observed. The Gaussians in the spectra of (2), (4) positioned at the lower frequency end of the spectral region, i.e., $G(i,3)_{i=2,4}$, have much lower amplitudes than those in Figs. S14, S15, i.e., $G(i,3)_{i=1,3}$. The decrease of the amplitude runs parallel with the smaller emission quantum yields of (2) and (4) compared to the quantum yields of (1) and (3), Table 3.

A reasonable explanation is that the emissive PNP-centered excited states of **(2)** and **(4)** of a lower energy undergo either or both a faster non-radiative relaxation to the ground state or convert to excited states such as the $MLCT_{Cu(I) \rightarrow L}$, L= phen, dmp, excited states.

Table 3. Luminescence quantum yields in deaerated CH_3CN and CH_2Cl_2 .

Compound	$\phi \times 10^3$	
	Solvent	
	CH_3CN	CH_2Cl_2
(1)	0.90	7.73
(2)	0.21	1.58
(3)	0.28	38.1
(4)	0.046	0.38

Solvent effects on the luminescence of the complexes were also investigated. A decrease in the luminescence quantum yields of all complexes results when CH_2Cl_2 solvent is replaced by CH_3CN , Table 3. This decrease is consistent with the quenching of the MLCT character of the respective emissive excited states by the coordinating solvent CH_3CN as previously described by McMillin *et al.*²⁸ Interestingly, the luminescence quantum yields of the complexes **(2)** and **(4)** are smaller than those of the complexes **(1)** and **(3)**. A likely explanation involves some degree of conversion of the emissive ligand-centered excited states of **(2)** and **(4)** to the MLCT excited states where the efficiency of the luminescence is smaller.

The complexes **(2)** - **(4)** also exhibit intense luminescence in the solid state, Fig. 11. In comparison to the emission spectra recorded when the complexes **(2)** - **(4)** were irradiated at λ_{exc}

= 330 nm in solution phase, those recorded in solid phase ($\lambda_{\text{exc}} = 370$ nm) have the maxima displaced to longer wavelengths and the bands remained asymmetric as they were in solution phase. In the best fittings of the (2) and (4) emission spectra, $\text{Adj-R}^2 \geq 0.9998$ and $\text{Reduce-}\chi^2 \leq 5 \times 10^{-5}$, small shoulders can be seen on the longer wavelength side, Figs. S18, S19. Their positions are near where the luminescence from the $\text{MLCT}_{\text{Cu(I)} \rightarrow \text{L}}$, L = dmp or phen, excited states were observed in solution phase.

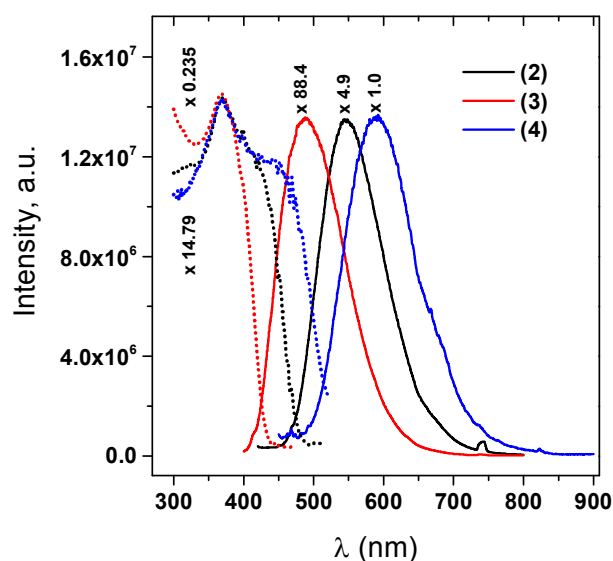


Figure 11. Solid state emission spectra of the PNP complexes (2)-(4) recorded at $\lambda_{\text{exc}} = 370$ nm (solid line) and their corresponding excitation spectra (dotted line). The latter were recorded at the maxima of the emission spectra. A key to the compounds and scale multiplying factors are given in the inset. Shoulders in the excitation spectra of (2) and (4) are observed at 407 and 417 nm, respectively

On this basis, they could be associated with the radiative relaxation of the respective $\text{MLCT}_{\text{Cu(I)} \rightarrow \text{L}}$, L = dmp or phen, in the solid phase. Support for this assignment comes from the

presence of shoulders in the excitation spectra of **(2)** ($\lambda \sim 407$ nm) and **(4)** ($\lambda \sim 417$ nm) but not in the spectrum of **(3)** and PNP-centered excited states of these complexes have been red-shifted with respect to their positions in solution, Figs. 10 and 11. In consequence there is a significant overlap of the metal to ligand transitions with the PNP-centered ones in the cumulative spectrum.

If the $\text{MLCT}_{\text{Cu(I)} \rightarrow \text{PNP}}$ charge transfer excited state in **(3)** remains at much larger energies as it is the case in solution phase, their contribution to the emission spectrum will be weak to vanishingly small compared to contributions from the PNP-centered excited states. On the basis of these arguments, it is possible to assign the $\lambda = 370$ nm ($\tilde{\nu} \sim 27$ kK) maximum in the excitation spectrum of **(3)** to an electronic transition from a PNP-centered excited state.

Table 4. Emission lifetimes of the PNP complexes recorded in the solid state.

compound	$\tau_{\text{em},1}$ (s)	$I_1(0)$, a.u.	$\tau_{\text{em},2}$ (s)	$I_2(0)$, a.u.	λ_{obs} (nm)
(2)	1.29×10^{-6}	0.286	8.93×10^{-6}	0.668	550
(3)	7.79×10^{-6}	0.375	4.59×10^{-5}	0.619	500
(4)	3.65×10^{-7}	0.155	2.18×10^{-6}	0.845	600

In contrast to the short-lived luminescence in solution, the intense luminescence of the complexes in solid phase span longer time scales, Table 4. These characteristics of the solid-state emission allowed a time-resolved study of the luminescence. Flash fluorescence traces were recorded at the wavelength of the maximum in the emission spectrum of **(2)**, **(3)** and **(4)**, Fig. 11. While the traces deviate significantly from a single exponential decay, $I(t) = I(0) \exp(-t/\tau_{\text{em}})$ where $I(t)$ and $I(0)$ are the relative emission intensities at t and zero times, they were correctly fitted to a double exponential decay, $I(t) = I_1(0) \exp(-t/\tau_{\text{em},1}) + I_2(0) \exp(-t/\tau_{\text{em},2})$, Table 4.

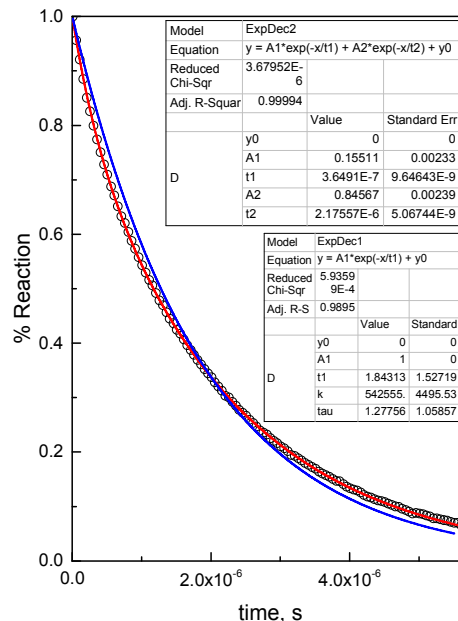


Figure 12. Typical mono (blue line) and biexponential (red line) fittings of the complex **(4)** luminescence decay (black circles). Inserts contain the statistic parameters of each fitness goodness.

A comparison of the single exponential and double exponential fitting is shown in Fig. 12, where the failure of the monoexponential fitting to capture the experimental data obtained with **(4)** is clearly seen. It is possible to associate $\tau_{em,1}$ with intraligand electronic transitions involving the PNP ligand and $\tau_{em,2}$ with the relaxation of $\rightarrow Cu \rightarrow L$, $L = dmp$ or $phen$, excited states of the **(2)** and **(4)** complexes. In contrast, the emission with a $\tau_{em,2}$ lifetime in **(3)** is much slower than in **(2)** and **(4)**. Because of the absence of $MLCT_{Cu \rightarrow L}$, $L = dmp$ or $phen$, excited states in **(3)** and the luminescence associated with them, it is possible to relate the lifetime τ_2 with radiative transitions from a stabilized $MLCT_{Cu(I) \rightarrow PNP}$ charge transfer excited state, Fig. 13, and also to PNP-centered electronic transitions. Conversely these PNP-centered and $MLCT_{Cu(I) \rightarrow PNP}$ charge transfer excited states are expected to be energetically close in compounds **(2)** and **(4)** and

cannot be differentiated from the convolution. The lower energy $\text{MLCT}_{\text{Cu(I)} \rightarrow \text{L}}$, L = phen or dmp, charge transfer excited states which were seen as shoulders of intense electronic transitions in the excitation spectra, Fig. 11, decay with a $\tau_{\text{em},2}$ lifetime.

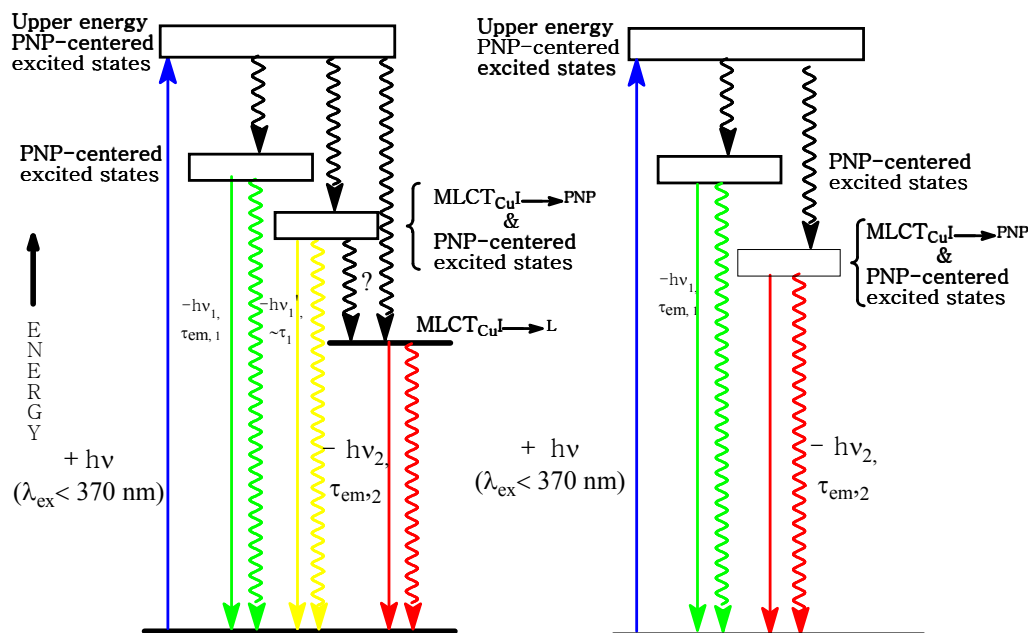


Figure 13. Energy diagram for the photophysical processes of **(2)** and **(4)**. Photonic energies reached when $\lambda_{\text{exc}} \leq 370$ nm correspond to PNP-centered upper energy excited states of **(2)** and **(4)**, left side figure, or **(3)**, right side figure. In the left side figure the possible conversion of majorly PNP excited states to $\text{MLCT}_{\text{Cu(I)} \rightarrow \text{L}}$, L = dmp or phen, excited states is marked with a question mark.

CONCLUSIONS

The combination of the PNP pincer ligand (PNP=N,N'-bis(diphenylphosphine)-2,6-diaminopyridine) and copper(I) where there is a strong tendency for four-coordinate complexation leads to a homoleptic Cu(I) complex $[\text{Cu}(\text{PNP-}\kappa\text{P}^I:\kappa\text{N}^I)_2]^+$ (**1**) that shows fluxional behavior in acetonitrile solution in which an intramolecular switch in the $-\text{PPh}_2$ that coordinates to the metal has an activation energy of 47.4 kJ/mol. Reaction of (**1**) with $[\text{Cu}(\text{I})\text{phen}]^+$ leads to the formation of a binuclear helicate $[\text{Cu}_2(\text{PNP})_2(\text{phen})]^{2+}$ (**2**) where the second copper ion is coordinated to the dangling $-\text{PPh}_2$ and phen ligand. The versatility of the PNP ligand is also shown by the formation of a mononuclear pincer complex $[\text{Cu}^{\text{I}}(\text{PNP})(\text{PPh}_3)]^+$ (**3**), where the PNP ligand is tridentate and a fourth coordination is formed with PPh_3 . In contrast with the reaction with $[\text{Cu}(\text{I})\text{phen}]^+$, the reaction with $[\text{Cu}(\text{I})\text{dmp}]^+$, where the dmp ligand has a propensity for tetrahedral coordination, leads to the heteroleptic complex $[\text{Cu}^{\text{I}}(\text{PNP-}\kappa\text{P}^I:\kappa\text{N}^I)(\text{dmp})]^+$ (**4**). This complex shows similar intramolecular fluxional behavior for the PNP ligand to that shown by (**1**). All four complexes exhibit emission in solution and, remarkably, complexes (**2**)-(4) display intense luminescence in the solid state. The emission lifetime traces were fitted as biexponential decays with time constants in the microsecond range. The radiative relaxation is ascribed to electronic transitions in both the ligand PNP and metal-to-ligand charge transfer (MLCT). These studies reveal that a mismatch of ligand and metal geometric constraints can lead to a diverse range of complexation behavior.

ASSOCIATED CONTENT

Supporting Information Available: Additional tables and figures for NMR characterization and fluxional behavior, and emission information in PDF file. X-Ray crystallographic files of **(1)-(4)** in CIF format (CCDC 1522539, 1522540, 1522541, 1522542).

AUTHOR INFORMATION

Corresponding Author

*G.F. e-mail: ferraudi.1@nd.edu

*L.L. e-mail: luis.lemus@usach.cl

ACKNOWLEDGMENTS

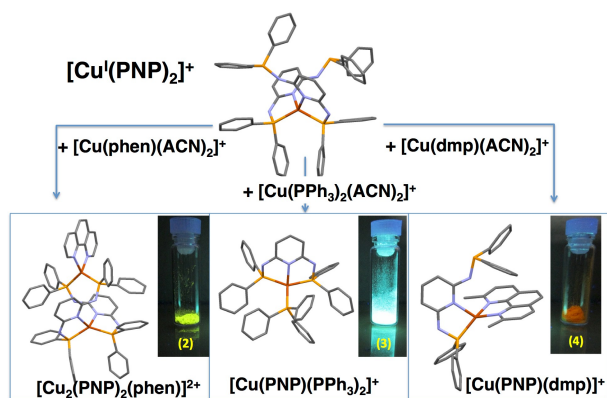
We thank FONDECYT Chile for financial support under project Fondecyt Iniciación N° 11130172. JG acknowledges Fondecyt N°1140193. Part of this work was carried out in the Notre Dame Radiation Laboratory (NDRL). The NDRL is supported by the Division of Chemical Sciences, Geosciences and Biosciences, Basic Energy Sciences, Office of Science, United States Department of Energy through grant number DE-FC02-04ER15533. This is the contribution number NDRL 2160.

REFERENCES

- 1 W. Dahlhoff, S. Nelson. *J. Chem. Soc. Inorg. Phys. Theor.* 1971, 2184.
- 2 C. Moulton, B. Shaw. *J. Chem. Soc., Dalton Trans.* 1976, **11**, 1020.
- 3 D. Benito-Garagorri, K. Kirchner. *Acc. Chem. Res.* 2008, **41**, 201.
- 4 H. Li., B. Zheng, K.W. Huang. *Coord. Chem. Rev.* 2015, **293**, 116.
- 5 M. Albrecht, G. van Koten. *Angew. Chem., Int. Ed.* 2001, **40**, 3750.
- 6 A. Vedernikov, P. Wu, J. Huffman, K. Caulton. *Inorg. Chim. Acta.* 2002, **330**, 103.
- 7 J. van der Vlugt, E. Pidko, D. Vogt, M. Lutz, A. Spek. *Inorg. Chem.* 2009, **48**, 7513.
- 8 C. Müller, E. A. Pidko., M. Lutz, A. L. Spek, D. Vogt. *Chem. Eur. J.* 2008, **14**, 8803.
- 9 A Hayashi, M. Okazaki, F. Ozawa, R. Tanaka. *Organometallics* 2007, **26**, 5246.
- 10 G. Rao, S. Gorelsky, I. Korobkov, D. Richeson. *Dalton Trans.* 2015, **44**, 19153.
- 11 D. Petrovic, T. Bannenberg, S. Randoll, P. Jones, M. Tamm. *Dalton Trans.* 2007, **26**, 2812.
- 12 Z. Pan, M. Gamer, P. Z. Roesky. *Z. Anorg. Allg. Chem.* 2006, **632**, 744.
- 13 S. Serin, F. Pick, G. Dake, D. Gates. *Inorg. Chem.* 2016, **55**, 6670.
- 14 W. Schirmer, U. Flörke, H. J. Haupt, H. J. Darstellung. *Z. Anorg. Allg. Chem.* 1987, **545**, 83.
- 15 A. Barbieri, G. Accorsi, N. Armaroli. *Chem. Commun.* 2008, **19**, 2185.
- 16 Y. J. Li, Z. Y. Deng, X. F. Xu, H. B. Wu, Z. X. Cao, Q. M. Wang. *Chem. Commun.* 2011, **47**, 9179.
- 17 H-C Liang, K. Karlin, R. Dyson, S. Kaderli. *Inorg. Chem.* 2000, **39**, 5884.
- 18 G. M. Sheldrick. *Acta Cryst.*, 2015, **A71**, 3.
- 19 G. M. Sheldrick. *Acta Cryst.*, 2015, **C71**, 3.
- 20 L. Yang, D. Powell, R. Houser. *Dalton Trans.* 2007, **9**, 955.

- 21 L. Lemus, J. Guerrero, J. Costamagna, G. Estiu, G. Ferraudi, A.G. Lappin, A. Oliver, B. Noll. *Inorg. Chem.* 2010, **49**, 4023.
- 22 S. Harkins, J. Peters. *J. Am. Chem. Soc.* 2005, **127**, 2030.
- 23 S. Harkins, J. Peters. *J. Am. Chem. Soc.* 2004, **126**, 2885.
- 24 The geometry of complex C is described as distorted tetrahedral, however, by inspection of the crystallographic data a seesaw geometry is more representative.
- 25 E. Abel, K. Orrell, A. Osborne, H. Pain. *J. Chem. Soc., Dalton Trans* 1994, **23**, 3441.
- 26 E. Riesgo, Y. Hu, F. Bouvier, R. Thummel. *Inorg. Chem.* 2001, **40**, 2541.
- 27 No experiments were done under 244K, because precipitation of the complex was observed and the consequent loss of signal resolution.
- 28 C. Palmer, D. Mcmillin, C. Kirmaier, D. Holten. *Inorg. Chem.* 1987, **26**, 3167.

Table of Contents.



The versatility of PNP ligand in coordinating to Cu(I) resulted in the formation of emissive complexes with notable structural differences.